DNA Damage in Embryonic Stem Cells Caused by Nanodiamonds

Yun Xing,[†] Wei Xiong,[†] Lin Zhu,[†] Eiji Ōsawa,[‡] Saber Hussin,[§] and Liming Dai[†,⊥,*]

[†]Department of Chemical and Materials Engineering, School of Engineering, University of Dayton, 300 College Park, Dayton, Ohio 45469, United States, [‡]NanoCarbon Research Institute, Ltd., Kashiwa, Chiba 277-0882, Japan, [§]AFRU711 HPW/RHPB, Wright-Patterson Air Force Base, Dayton, Ohio 45433, United States, and [⊥]Department of Chemical Engineering, Case School of Engineering, Case Western Reserve University, Cleveland, Ohio 44106, United States

ABSTRACT Because of their unique photoluminescence and magnetic properties, nanodiamonds (NDs) are promising for biomedical imaging and therapeutical applications. However, these biomedical applications will hardly be realized unless the potential hazards of NDs to humans and other biological systems are ascertained. Previous studies performed in our group and others have demonstrated the excellent biocompatibility of NDs in a variety of cell lines without noticeable cytotoxicity. In the present paper, we report the first genotoxicity study on NDs. Our results showed that incubation of embryonic stem cells with NDs led to slightly increased expression of DNA repair proteins, such as p53 and MOGG-1. Oxidized nanodiamonds (O-NDs) were demonstrated to cause more DNA damage than the pristine/raw NDs (R-NDs), showing the surface chemistry specific genotoxicity. However, the DNA damages caused by either the O-NDs or the R-NDs are much less severe than those caused by multiwalled carbon nanotubes (MWNTs) observed in our previous study. These findings should have important implications for future applications of NDs in biological applications.

KEYWORDS: nanodiamond · DNA damage · embryonic stem cells · cytotoxicity · genotoxicity

Nanodiamonds (NDs) are a relatively new class of carbon nanomaterials that have the diamond-like structure at a nanometer scale. Like carbon nanotubes and fullerene C_{60}, NDs also possess unique optoelectronic, mechanical, thermal, and biological properties attractive for a variety of important applications, including nanomedicine.[1] Of particular interests are their strong near-infrared (NIR) photoluminescence[2] and magnetic properties,[3] which make NDs a promising alternative to the current bioimaging platforms. The strong photoluminescence emission associated with the pristine/raw NDs (R-NDs) has been attributed to their surface defects/surface declocalization of π electrons (for 5 nm particles or smaller) and/or color vacancy (N-V) centers inside the nanoparticle (for 100 nm particles or so).[4] NDs treated by high energy beam to create more color centers[5,6] or conjugated with fluorescent dyes to enhance the fluorescence intensity[7,8] are particularly useful for fluorescence imaging inside living cells. Besides, the N-V defect centers also impart magnetic properties to NDs to render them feasible for single-electron spin imaging, as demonstrated recently by Balasubramanian and co-workers.[9] More recently, Manus *et al.*[10] reported a 10-fold MRI contrast enhancement with a Gd(III)−ND conjugate as compared to the monomer Gd(III) complex. Furthermore, NDs and their derivatives (notably oxidized NDs) have also been proved useful for protein immobilization, biopurification, bioseparation, drug delivery,[11−13] and biosensing, due to their high surface area and strong affinity to proteins.[14−17]

On the other hand, the biomedical applications will hardly be realized unless the potential hazards of NDs to humans and other biological systems are ascertained. We have previously investigated the biocompatibility (cyctotoxicity) of NDs on macrophage and neuroblastoma cells.[18,19] Our results indicated that NDs did not produce a significant amount of reactive oxygen species (ROS) and did not affect the mitochondrial function and ATP production of these cells. The biocompatibility of NDs at the cellular level has been confirmed by independent studies.[7,20] For instance, Vial *et al.*[7] incubated peptide-grafted NDs with cultured Chinese hamster ovarian (CHO) cells for up to 72 h and observed no adverse effect on intracellular dehydrognase activity even at a dose of 40 μg/mL. Although these initial results are in favor of NDs for biomedical applications, more comprehensive and thorough studies are needed to exploit the full potentials of NDs for biomedical applications. It is now well-known that careful scrutiny of the toxicity of nanomaterials at the molecular level is needed even for materials that seem to be benign and cause limited or minimal toxicity at the cellular level.[21] However, the genotoxicity of NDs

* Address correspondence to liming.dai@case.edu.

Received for review January 22, 2011 and accepted February 18, 2011.

Published online March 03, 2011
10.1021/nn200279k

remains largely unknown. In the present study, we carried out an investigation of the possible effects of NDs on DNA damage of mouse embryonic stem (ES) cells.

ES cells are a unique cell population with the ability to undergo both self-renewal and differentiation with the potential to give rise to all cell lineages and an entire organism.[22,23] It has been shown that ES cells are highly sensitive to DNA damages, possibly caused by UV irradiation[24] or exposure to nanoparticles (*e.g.*, multiwalled carbon nanotubes, MWNTs).[21] The sensitivity of ES cells to DNA damage prompted us to study the genotoxicity of NDs in mouse ES cells, while the well-established methodologies reported in our previous paper[21] for characterizing DNA damages of ES cells made the ES as the cell of choice.

RESULTS

A fluorescent Western blotting kit (Westerndot, Invitrogen Cat# W10132) was used for the protein expression analysis. Briefly, the samples were blotted with biotinylated secondary antibodies after primary antibody incubation. After washing, QD605—streptavidin conjugates were applied to the PVDF membranes for about 1 h. Thereafter, the QD-stained membranes were washed in buffer several times and imaged in a transilluminator using 302 nm UV light to excite the fluorophore. DNA damage biomarkers, including p53 (short-time response, 2 and 4 h treatments), DNA double band breaks marker (MOGG-1), and two DNA repair markers Rad51 (recombinatorial repair) and XRCC-4 (nonhomogeneous end joining), are studied. For each of the biomarkers, a β-actin blot was also included for quantification purposes. The p53 is a DNA repair protein (53 kD) that remains inactive under normal conditions and becomes active upon DNA damage caused by irradiation, oxidative stress, *etc.* Therefore, a transient increase in p53 expression is often seen at the beginning of DNA damage. Our Western blotting results showed that incubation with both the R-NDs and O-NDs resulted in a slight increase in p53 expression in the short term (2 and 4 h, Figure 1a). While the increase in p53 expression was more obvious at 2 h and became less at 4 h for the R-NDs, the cells treated by O-NDs under the same condition showed increasing p53 expression with time. Thus, different DNA damage dynamics were observed for the two different types of NDs. In both cases, the increases in p53 expression were more profound at the low dose (5 μg/mL) as compared to the high dose (100 μg/mL). Within a relatively short incubation time (*e.g.*, 2 h), the expression of other downstream DNA repair proteins, such as MOGG-1 and Rad 51, was insignificant with regard to the baseline level (Figure 1a).

Prolonged incubations (*e.g.*, 4—24 h), however, caused a significant increase in MOGG-1 expression for the O-NDs (but not the R-NDs, Figure 1b), albeit much lower than that caused by the positive reference (CdO) or MWNT. Along with the increase in MOGG-1, the sample treated with O-NDs also showed an elevated expression of Rad51, indicating an ongoing recombinatorial repair. The dosage-dependent p53 expression for different types of NDs given in Figure 1c suggests that O-NDs caused more DNA damage than R-NDs, albeit both show much less DNA damage than MWNTs. Nevertheless, none of the treatments seemed to cause any significant change in the XRCC-4 expression. Similar to the pattern in p53 expression at relatively short time (*e.g.*, 2—4 h, Figure 1a), more DNA double-strand damage (as indicated by MOGG-1, Figure 1b) was observed at the low dose with respect to the high dose (100 μg/mL). To test this point, we used a series of O-NDs with concentrations (the O-NDs were selected due to their more profound effect) ranging from 2.5, 5, 10, 50, to 100 μg/mL and analyzed their MOGG-1 expression. It was confirmed that the lower dosage (2.5 and 5 μg/mL) caused more MOGG-1 production than the higher dosages (Figure 2). Although further studies are needed to understand the exact DNA damage mechanism, the aggregation of nanoparticles may have played an important role since NDs do not dissolve well in the aqueous cell culture media. Optical microscopic images showed that NDs formed aggregates in cell culture media (Figure 2). The number of aggregates and the size of individual clusters both increase as the concentration of O-ND increases. Scanning microscopic images showed that the size of the clusters ranges from about 100 nm up to a few micrometers (*vide infra*). The bigger the aggregates formed at the higher doses, the more difficult for them to get into the cell to cause the DNA damage.

In addition to DNA repair proteins, we have also studied the effects of NDs on the ES cell differentiation. The undifferentiated state of ES cells can be characterized by a high level of expression of alkaline phosphatase (AP) and the expression of transcription factor Oct-4. AP activity was determined by using the alkaline phosphatase detection kit (Millipore, Catalog# SCR004) containing naphthol and fast red violet. The level of AP activity is indicated by the intensity of the pink color. AP staining results showed that ES cells treated with R-NDs remained mostly undifferentiated as their AP activity level was as high as that in untreated ES cells (Figure 3a). However, the O-NDs did cause the ES cell differentiation, as shown by the significant reduction in the AP activity (Figure 3b). The effect was most profound at the low dosage (very faint pink color). Oct-4 is a homeodomain transcription factor of the POU family and is critically involved in the self-renewal of undifferentiated embryonic stem cells.[21] Abnormal expression (either too much or too little) of Oct-4 often signals the

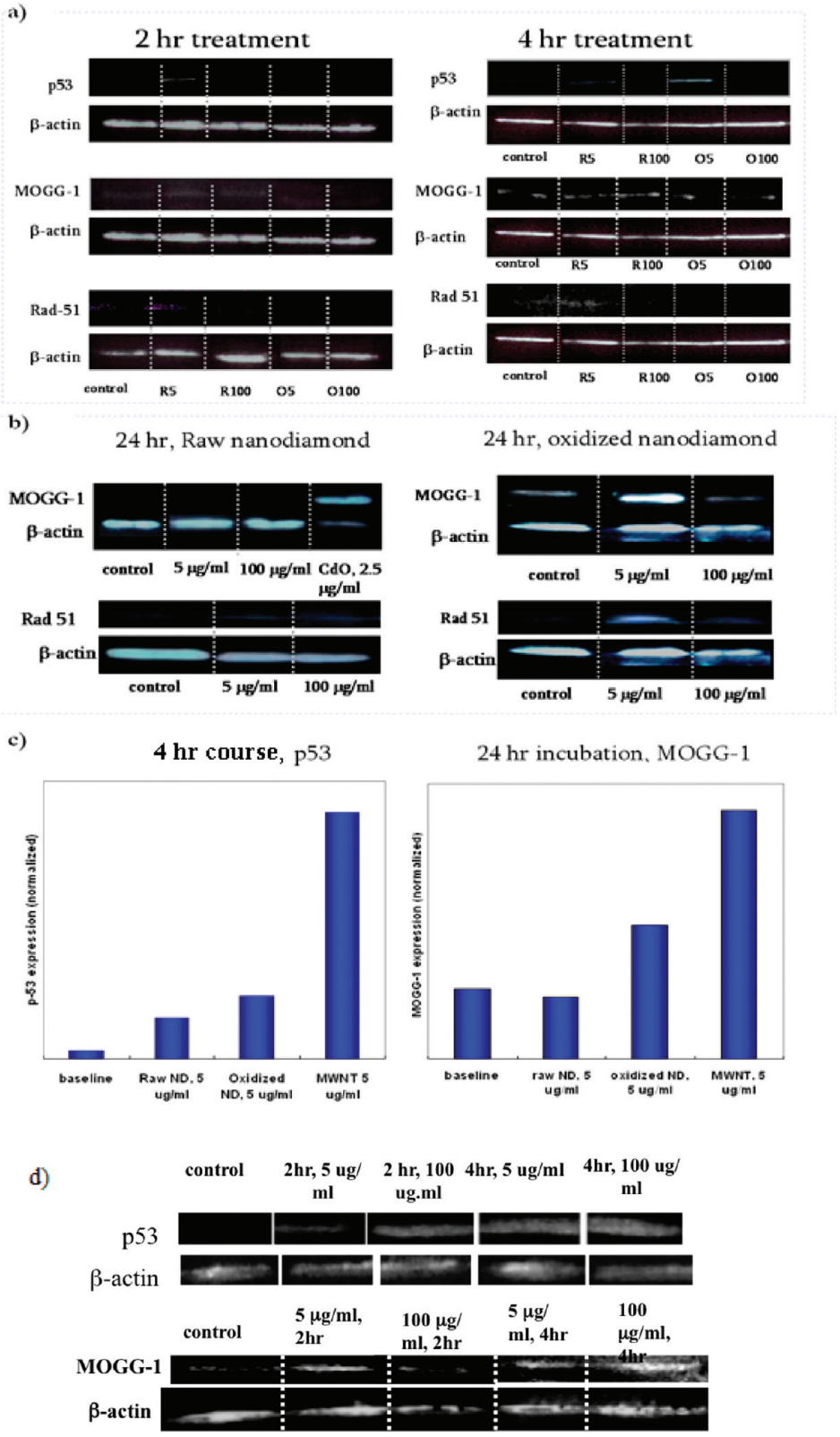

Figure 1. (a) Short-term responses as shown in p53, MOGG-1, and Rad-51. Note that R5, R100, O5, and O100 represent R-NDs at 5 μg/mL, R-NDs at 100 μg/mL, O-NDs at 5 μg/mL, and O-NDs at 100 μg/mL, respectively. (b) Longer term response, 24 h incubation; (c) quantified DNA damage (as in protein expression) compared with MWNTs. (d) Responses in p53 and MOGG-1 from MWNT samples in ES cells.

differentiation of ES cells. Our Western blotting of Oct-4 (primary antibody, Santa Cruz, Cat# sc-5279) showed an increase of this protein in cells treated with the O-NDs, but not with the R-NDs.

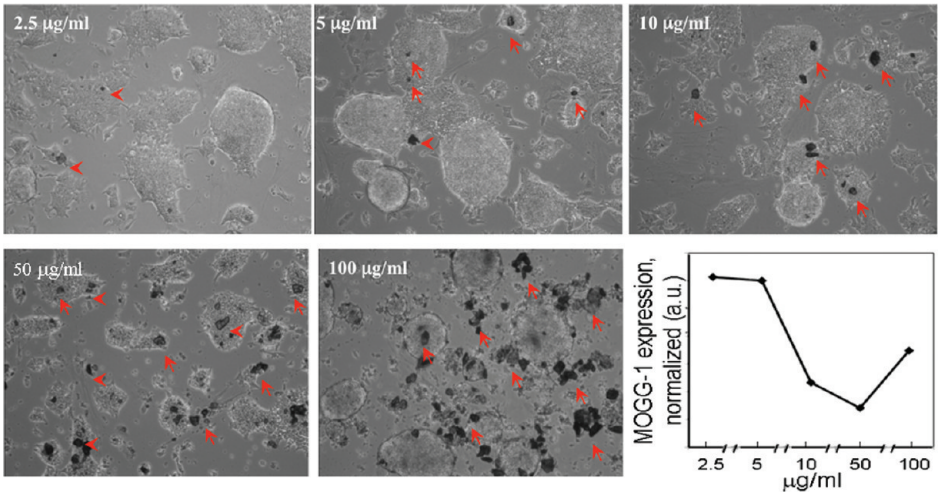

Figure 2. Aggregates are indicated by arrows. As the amount of NDs increases, the number and size of aggregates increased too. The graph shows MOGG-1 expression as a function of dose, showing that the lower doses (2.5 and 5 μg/mL) caused more damage than the higher doses due to the formation of aggregates to inhibit the entry of NDs into cells (see text).

Annexin V staining is used to detect cells that have expressed phosphatidylserine on the cell surface, a feature found in apoptosis as well as other forms of cell death.[21] In the present study, Annexin V−FITC conjugates (Invitrogen, Catalog# PHN1010) were used to detect apoptotic cells. ES cells were incubated with NDs for 24 h and then stained with Annexin V−FITC (green fluorescence). Thereafter, cell nuclei were counterstained with DAPI (blue fluorescence) and imaged with an epifluorescence microscope. As can be seen in Figure 3c, the R-NDs seemed to be quite benign to ES cells since no significant amount of Annexin V staining (green) was observed at either 5 or 100 μg/mL. In contrast, cells treated with the O-NDs showed very strong green fluorescence, especially in the low dosage group (Figure 3c, lower panel), indicating ongoing apoptosis process caused, once again, by the uptake of small NDs.

To examine the aggregated state of NDs and possible mechanical damages to the ES cells caused by the ND clusters, we grew ES cells on gelatin-treated glass coverslips in the presence of NDs (the pristine and oxidized for 24 h) for SEM investigation. Briefly, the cells were fixed with 2.5% glutaraldehyde (primary fixation) and then 1% osmium tetroxide (secondary fixation) and sputter-coated with gold prior to imaging. As shown in Figure 4, it is clear that NDs formed clusters of a few hundred nanometers to several micrometers in size (indicated by arrows) and stuck onto the cell membrane. There was no apparent difference between the O-NDs and R-NDs. The fact that these clusters stay attached to the cells after many rounds of washing during the sample preparation implies strong interactions between the nanoparticle and the cell membrane. No obvious structural damage (holes or fractures in the membrane) was observed, though some local/regional cell deformation (*e.g.*, change in curvature) caused by the mechanical load of NDs cannot be ruled out.

We have also used confocal microscopy to investigate the internalization of nanodiamond into ES cells. For confocal microscope imaging, amine-functionlized NDs (primary particles 4−5 nm) were conjugated with Cy5.5 (GE Life Sciences) and incubated with ES cells for 24 h, followed by washing with PBS before being fixed with 3.7% formaldehyde. For nuclear counterstaining, Syto-16 was then added to the cells before fixation. Thereafter, cytoskeleton structure was outlined by staining β-actin with Alexa 555. After all of the staining steps, the cells were viewed under confocal microscope with no counterstaining (one color, ND-Cy5.5), DNA counterstained (2 colors, Cy5.5 and Syto-16), or DNA and β-actin both counterstained (3 colors, Cy5.5, Syto-16, and Alexa 555). Our results showed that NDs were indeed engulfed by ES cells and some of the intracellular NDs remained mainly in the cytoplasm, but not in the nucleus (Figure 5).

DISCUSSION

Our results showed that NDs caused increased expression of DNA repair proteins in mouse ES cells, indicating the occurrence of DNA damage. It was found that the R-NDs caused a slight and transient increase in p53 expression within 2−4 h of cell incubation. However, no significant change in downstream biomarkers has been found in ES cells treated with the R-NDs, suggesting that the damage is minor and might have been repaired very quickly. Similar treatment with the O-NDs also led to an increased expression of p53. Longer incubation (24 h) revealed increased expression of MOGG-1, indicating the breakage of DNA double strands. Additional experiments on apoptosis and ES cell differentiation showed that the R-NDs were quite benign to ES cells and did not cause increased

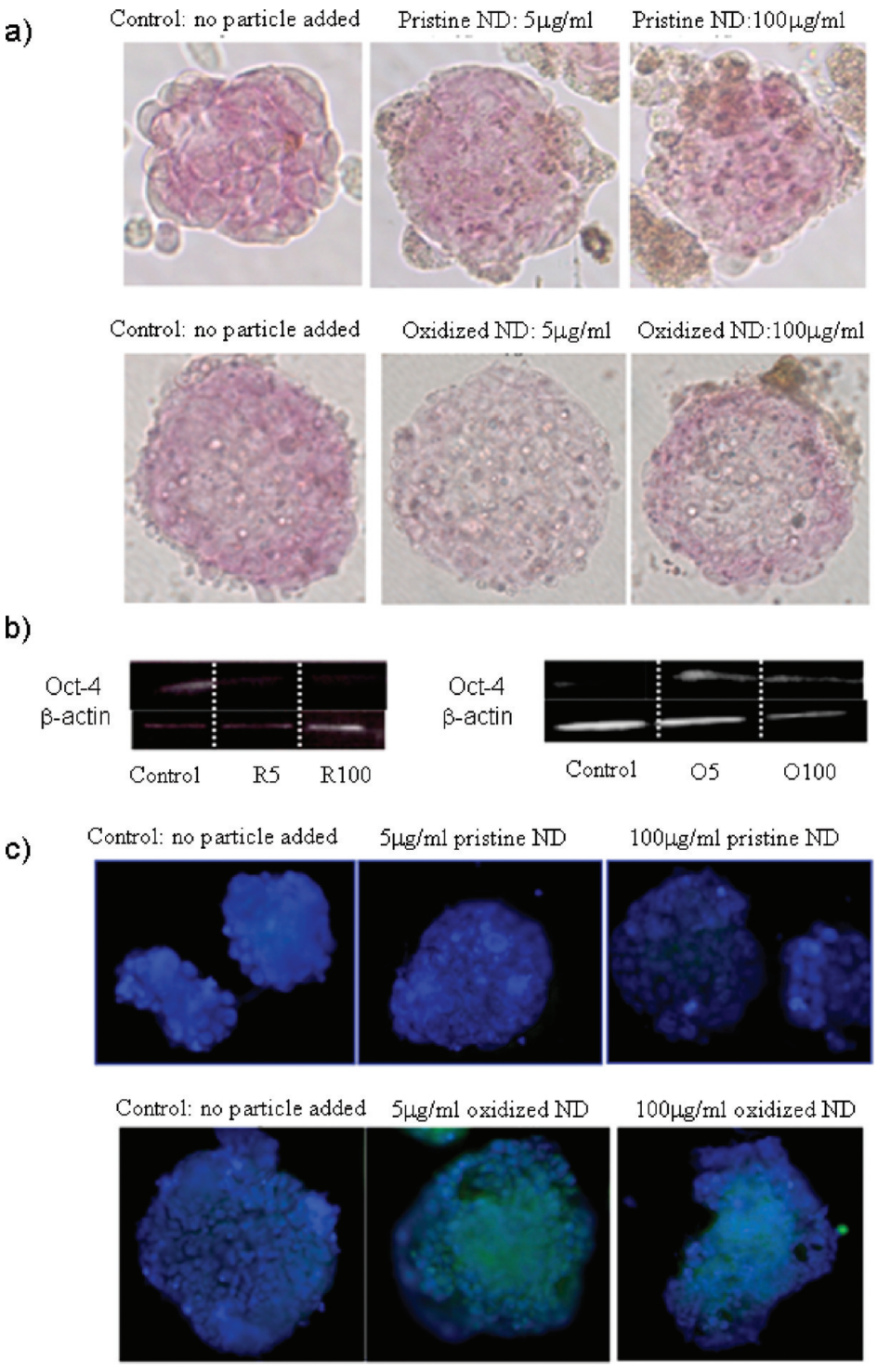

Figure 3. (a) Alkaline phosphatase staining of ES cells treated with nanodiamond for 24 h; (b) Oct-4 Western blotting of ES cells treated with pristine nanodiamonds (R-NDs) and oxidized nanodiamonds (O-NDs); (c) Annexin V staining of ES cells treated with the nanodiamonds.

differentiation or noticeable apoptosis. However, ES cells treated with the O-NDs showed signs of differentiation (loss of AP activity and increases in Oct-4 expression), as well as apoptosis (Annexin V positive). These findings seem to be in disagreement with the findings by Liu *et al.*,[25] in which they claimed that NDs do not interfere with the gene expression of cultured embryonic fibroblasts. This inconsistency could be explained by the difference in cell types. Although both are embryonic, the ES cells are much more sensitive to DNA damaging agents than the embryonic fibroblasts, as we previously reported.[21]

SEM imaging showed that nanodiamonds at the high dose media formed clusters and stuck onto the

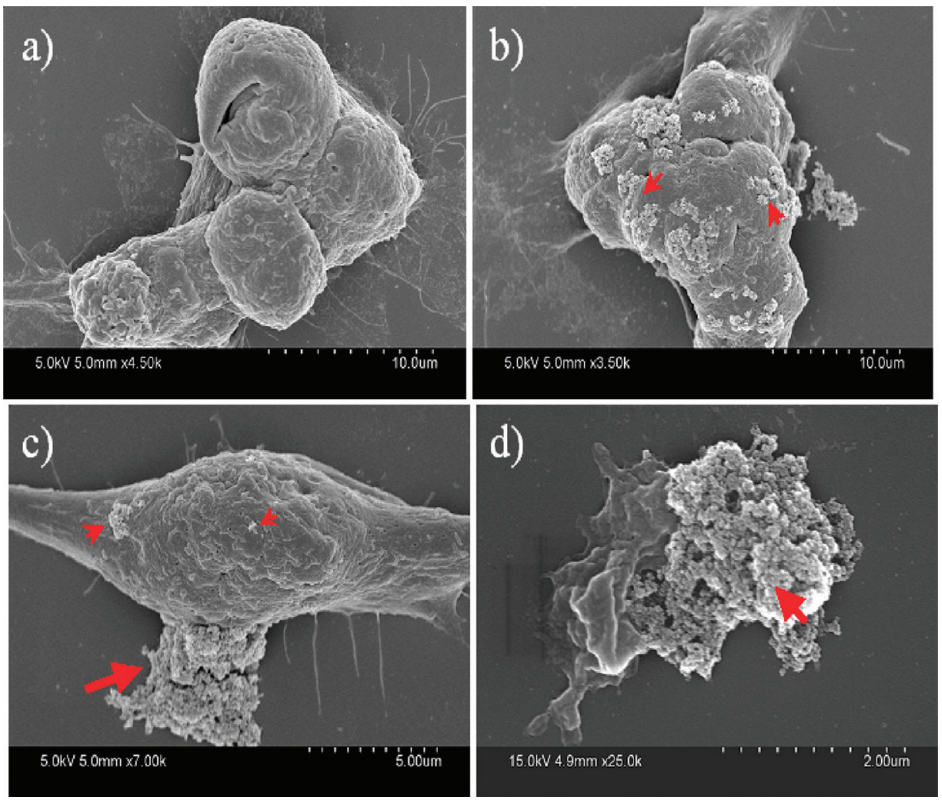

Figure 4. SEM images show that (a) the cell with no NDs attached, (b) a cell extensively covered with ND clusters, (c) a cell with ND clusters of various sizes, and (d) a collapsed cell under the huge ND cluster. Arrows indicate ND cluster; not all clusters are indicated.

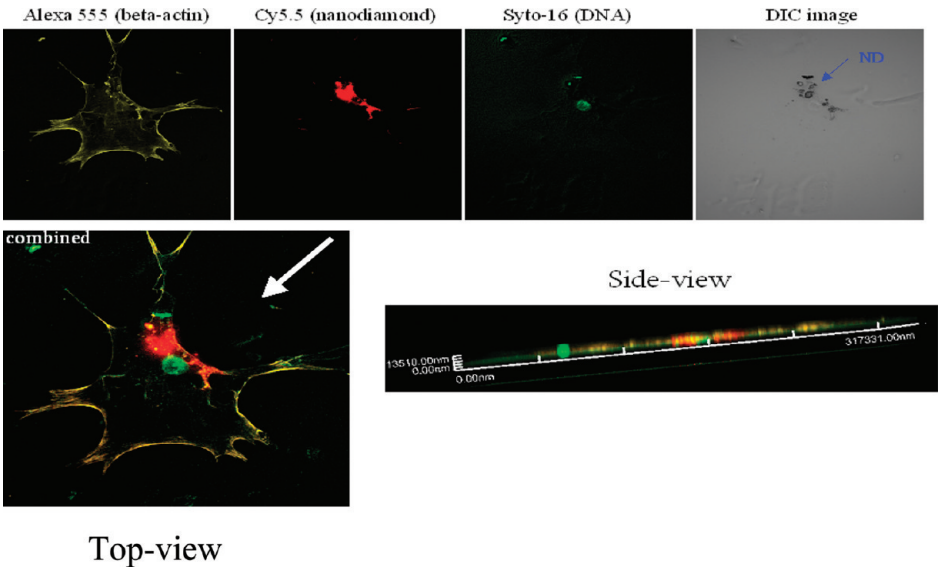

Figure 5. Confocal microscopy image of ES cells incubated with nanodiamonds. β-Actin was stained yellow with Alexa 555; NDs were conjugated to Cy5.5 (shown as red); and cell nuclei were stained with Syto-16 (green). Top-view image shows that the particles remained in the cytoplasm/perinuclear region, but did not enter the nucleus. Side-view image shows that signals (red) from the nanoparticles were in the same plane as signals (yellow) from β-actin, indicating that the particles were internalized.

cell membrane even after many rounds of washing. Some of the intracellular ND aggregates remained mainly in the cytoplasm with no sign of nuclear entry, consistent with findings from other research groups.[25,26] The more profound DNA damages caused by the O-NDs could arise from the differences in surface chemistry (negatively charged with carboxyl groups). Indeed, it has been reported that

nanoparticles with different surface chemistries showed different bioactivities[27] and different nonspecific absorption behaviors.[28,29] However, the possibility for more O-NDs to enter into the cell with respect to R-NDs under the same condition cannot be ruled out as O-NDs are more soluble and hence less aggregated. Although it is well-established that NDs can spontaneously enter cells,[6,30,31] recent studies have just emerged to shine some light onto the exact mechanism.[25,26] Given that NDs are known to have strong affinity to proteins,[15,16] it is likely that NDs could develop some kind of strong noncovalent bonds with cell surface proteins to be engulfed into cells. Indeed, we have seen from the SEM images many ND clusters clung onto the cell membrane. Due to their heterogeneous size distribution (4−5 nm primary particles and up to micro size clusters), it is highly possible that multiple endocytotic pathways are involved; for instance, a study by Liu *et al.*[25] suggested macropinocytosis and clathrin-dependent endocytosis for bigger particles (~100 nm) and caveolae-dependent uptake for particle size of 60 nm. Intracellular NDs are mostly localized in the cytoplasm with no sign for nuclear entry. The primary particles of 4−5 nm in size can readily form clusters in aqueous media particularly at high concentrations, which are often too big (a few hundred nanometers to a few micrometers) to pass through the nuclear pores.[32−34] Therefore, the possible DNA damage reflected by the observed activation of DNA repair proteins is likely caused by indirect mechanisms through, for example, the generation of ROS to interact with the DNA.[35] We have previously reported that NDs did not generate a significant amount of ROS in macrophage and neuroblastoma cells.[18,19] Since each cell type responds differently and ES cells are especially fragile, however, the possibility of ROS-induced damage cannot be excluded in this study.

CONCLUSIONS

In summary, we have, for the first time, demonstrated that nanodiamonds can activate DNA repair proteins in ES cells, suggesting possible DNA damages. The observed changes are more pronounced for the oxidized nanodiamonds (O-NDs) as compared to the pristine/raw NDs (R-NDs). Overall, the DNA damaging effects observed in the present study for both the O-NDs and R-NDs are much less severe than that previously reported for other carbon nanomaterials, such as MWNTs.[21] However, these findings do suggest some cautions need to be taken in future biomedical applications of NDs.

METHODS

Nanodiamonds. The pristine nanodiamond particles (4−5 nm) synthesized from the detonation method were obtained from NanoCarbon Research Institute Ltd. (Shinshu University, Japan). Details on the preparation and purification of these nanioparticles can be found in a previous publication by Kruger *et al.*[36,37]

Oxidization. Nanodiamond powders were carboxylated and oxidized following the procedures previously reported by Ushizawa *et al.*, and Kruger *et al.*[38,39] Briefly, the as-received nanodiamond powder (100 mg) was subjected to the treatment with concentrated acid (70% HNO_3 and 98% H_2SO_4 at a ratio of 1:3) in a sonication bath (model 75D, VWR) for 3 h and then stirred at 140 °C for 2 days, followed by stirring in 0.1 M NaOH aqueous solution at 90 °C for 2 h, and in 0.1 M HCl aqueous solution at 90 °C for 2 h. Any excess acids, bases, or impurities were extensively removed by repeated sonication, centrifugation, and decantion. Finally, the carboxylated/oxidized nanodiamonds were dried in the vacuum oven overnight.

Cell Culture and Treatment with Nanodiamonds. Mouse embryonic stem cells were purchased from Millipore (EmbryoMax Embryonic Stem Cell Line, strain C57/BL6, passage 11, normal male genotype, Cat# CMTI-2) and cultured according to the instructions provided by the supplier. ES cells were grown on gelatin-treated 6-well tissue culture plates in DMEM media (Gibco, Cat# 11965) supplemented with 10% ES quality FBS, LIF (10^6 unit per 500 mL, Millipore), non-essential amino acids (1×), L-glutamine (1×), penicillin-streptomycin (1×), and β-mercaptoethanol (5 μL in 500 mL). Nanodiamonds (pristine and oxidized) were added to the cells according to the dose (5 or 100 μg/mL) and incubated for 24 h before collection for subsequent analyses.

Western Blotting. After the treatment with NDs, the ES cells were harvested and lysated in RIPA buffer (150 mM NaCl, 1% NP-40, 0.05% deoxycholic acid, 1% SDS, 50 mM Tris (pH 7.4)) in the presence of protease inhibitors (Roche). Western blot was used to analyze the stem cell factor Oct-4 (Santa Cruz, sc-5279) and cell cycle checkpoint protein p53 expression level by probing with an anti-p53 monoclonal antibody (CalBiochem, Cat# OP03). The cell lysates were also probed with antibodies for DNA repair proteins OGG1 (alpha4diagnostics, mOGG13-A), Rad 51 (Santa Cruz, sc-56212), and XRCC4 (Santa Cruz, sc-8285).

The Annexin V−FITC staining followed the instruction of the manufacturer (Invitrogen, Cat# PHN1010). The images were captured by an inverted microscope (Olympus CK2) at 10× and 20× (oil) magnification and Olympus Fluoview scanning confocal microscope.

An AP detection kit (Millipore, Cat# SCR004) was used to examine the differentiation state of ES cells after being treated with NDs. The cells were cultured on gelatin-treated thin-bottom 8-well chamber slides (Labtek) and allowed to grow for 1 day before the treatment with NDs. After the treatment for 24 h, medium was aspirated and the cells were with 4% paraformaldehyde for 1−2 min. The cells were then rinsed with rinse buffer and incubated with AP stain solution (mixture of fast red violet (2 parts), naphthol (1 part), and DI water (1 part)) for 15 min at room temperature in the dark.

Scanning Electron Microscopy of ES Cells Treated with Nanodiamond. ES cells were cultured on gelatin-treated coverslips in the presence of nanodiamond for 24 h. After aspirating off the media and washing with PBS three times (5 min each), the ES cells were fixed with 2.5% glutaraldehyde (primary fixation) for 30 min at room temperature and stained with 1% osmium tetroxide (secondary fixation, EM Sciences, Cat#19160), followed by steps including dehydration in series of ethanol (increasing concentration from 25, 50, 75, 90, to 100%) and air drying. Prior to imaging by SEM, the glass coverslips were mounted onto a SEM stub with double adhesive tape and sputter-coated with gold.

Confocal Microscopy. ES cells were grown on gelatin-treated glass coverslips and incubated with NDs conjugated with

Cy5.5 (GE Life Sciences). After 24 h incubation, medium (containing the free nanoparticles) was aspirated off and the cells were washed three times with buffer. Thereafter, the cells were incubated with Syto-16 (1:10000 dilution, Invitrogen, S7578) for 30 min to counterstain cell nuclei. After washing with buffer three times (each for 5 min), the cells were then fixed with 3.7% formaldehyde/Triton X-100 for 15 min before staining for β-actin. β-Actin was stained with mouse anti-β-actin monoclonal antibody (Santa Cruz, sc-69879) at 1:50 dilution for 1 h and then with Alexa 555−goat anti-mouse secondary antibody conjugate (1:400, Invitrogen, A31621) for 30 min. Finally, the coverslips were mounted onto a glass slide before viewing under an inverted confocal microscope (Olympus Fluoview).

Acknowledgment. We thank L. Au, Y. Liu, Y. Hong, and M. Lunn for their help and are grateful to AFOSR (FA2386-10-1-4071) and Henry M. Jackson Foundation (CON115620) for financial support.

REFERENCES AND NOTES

1. Xing, Y.; Dai, L. Nanodiamonds for Nanomedicine. *Nanomedicine* **2009,** *4*, 207–218.
2. Davies, G; Hamer, M. F. Optical Studies of the 1.945 eV Vibronic Band in Diamond. *Proc. R. Soc. London, Ser. A* **1976,** *348*, 285–298.
3. Gruber, A.; Dräbenstedt, A.; Tietz, C.; Fleury, L.; Wrachtrup, J.; von Borczyskowski, C. Scanning Confocal Optical Microscopy and Magnetic Resonance on Single Defect Centers. *Science* **1997,** *276*, 2012–2014.
4. Chung, P. H.; Perevedentseva, E.; Cheng, C. L. The Particle Size-Dependent Photoluminescence of Nanodimonds. *Surf. Sci.* **2007,** *601*, 3866–3870.
5. Yu, S. J.; Kang, M. W.; Chang, H. C.; Chen, K. M.; Yu, Y. C. Bright Fluorescent Nanodiamonds: No Photobleaching and Low Cytotoxicity. *J. Am. Chem. Soc.* **2005,** *127*, 17604–17605.
6. Fu, C. C.; Lee, H. Y.; Chen, K.; Lim, T. S.; Wu, H. Y.; Lin, P. K.; Wei, P. K.; Tsao, P. H.; Chang, H. C.; Fann, W. Characterization and Application of Single Fluorescent Nanodiamonds as Cellular Biomarkers. *Proc. Natl. Acad. Sci. U.S.A.* **2007,** *104*, 727–732.
7. Vial, S.; Mansuy, C.; Sagan, S.; Irinopoulou, T.; Burlina, F.; Boudou, J. P.; Chassaing, G.; Lavielle, S. Peptide-Grafted Nanodiamonds: Preparation, Cytotoxicity and Uptake in Cells. *ChemBioChem* **2008,** *9*, 2113–2119.
8. Chang, I. P.; Hwang, K. C.; Chiang, C. S. Preparation of Fluorescent Magnetic Nanodiamond and Cellular Imaging. *J. Am. Chem. Soc.* **2008,** *130*, 15476–15481.
9. Balasubramanian, G.; Chan, I. Y.; Kolesov, R.; Al-Hmoud, M.; Tisler, J.; Shin, C.; Kim, C.; Wojcik, A.; Hemmer, P. R.; Krueger, A.; *et al.* Nanoscale Imaging Magnetometry with Diamond Spins under Ambient Conditions. *Nature* **2008,** *455*, 648–651.
10. Manus, L. M.; Mastarone, D. J.; Waters, E. A.; Zhang, X.; Schultz-Sikma, E. A.; MacRenaris, K. W.; Ho, D.; Meade, T. J. Gd(III)−Nanodiamond Conjugates for MRI Contrast Enhancement. *Nano Lett.* **2010,** *10*, 484–489.
11. Huang, H.; Pierstorff, E.; Osawa, E.; Ho, D. Active Nanodiamond Hydrogels for Chemotherapeutic Delivery. *Nano Lett.* **2007,** *7*, 3305–3314.
12. Liu, K. K.; Zheng, W. W.; Wang, C. C.; Chiu, Y. C.; Cheng, C. L.; Lo, Y. S.; Chen, C.; Chao, J. I. Covalent Linkage of Nanodiamond−Paclitaxel for Drug Delivery and Cancer Therapy. *Nanotechnology* **2010,** *21*, 315106.
13. Li, J.; Zhu, Y.; Li, W.; Zhang, X.; Peng, Y.; Huang, Q. Nanodiamonds as Intracellular Transporters of Chemotherapeutic Drug. *Biomaterials* **2010,** *31*, 8410–8418.
14. Bondar, V. S.; Pozdnyakova, I. O.; Puzyr, A. P. Applications of Nanodiamonds for Separation and Purification of Proteins. *Phys. Solid State* **2004,** *46*, 758–760.
15. Kong, X. L.; Huang, L. C. L.; Hsu, C. M.; Chen, W. H.; Han, C. C.; Chang, H. C. High-Affinity Capture of Proteins by Diamond Nanoparticles for Mass Spectrometric Analysis. *Anal. Chem.* **2005,** *77*, 259–265.
16. Yeap, W. S.; Tan, Y. Y.; Loh, K. P. Using Detonation Nanodiamond for the Specific Capture of Glycoproteins. *Anal. Chem.* **2008,** *80*, 4659–4665.
17. Zhao, W.; Xu, J. J.; Qiu, Q. Q.; Chen, H. Y. Nanocrystalline Diamond Modified Gold Electrode for Glucose Biosensing. *Biosens. Biotechnol.* **2006,** *22*, 649–655.
18. Schrand, A. M.; Huang, H.; Carlaon, C.; Schlager, J. J.; Osawa, E.; Hussain, S. M.; Dai, L. Are Nanodiamonds Cytotoxic?. *J. Phys. Chem. B* **2007,** *111*, 2–7.
19. Schrand, A. M.; Dai, L.; Schlager, J. J.; Hussain, S. M.; Osawa, E. Differential Biocompatibility of Carbon Nanotubes and Nanodiamonds. *Diamond Relat. Mater.* **2007,** *16*, 2118–2123.
20. Vaijayanthimala, V.; Tzeng, Y.-K.; Chang, H.-C.; Li, C.-L. The Biocompatibility of Fluorescent Nanodiamonds and Their Mechanism of Cellular Uptake. *Nanotechnology* **2010,** *20*, 425103.
21. Zhu, L.; Chang, D. W.; Dai, L.; Hong, Y. DNA Damage Induced by Multiwalled Carbon Nanotubes in Mouse Embryonic Stem Cells. *Nano Lett.* **2007,** *7*, 3592–3597.
22. Odorico, J. S.; Kaufman, D. S.; Thomson, J. A. Multilineage Differentiation from Human Embryonic Stem Cell Lines. *Stem Cells* **2001,** *19*, 193–204.
23. Watt, F. M.; Hogan, B. L. Out of Eden: Stem Cells and Their Niches. *Science* **2000,** *287*, 1427–1430.
24. Lin, T.; Chao, C.; Saito, S.; Mazur, S. J.; Murphy, M. E.; Appella, E.; Xu, Y. p53 Induces Differentiation of Mouse Embryonic Stem Cells by Suppressing Nanog Expression. *Nat. Cell Biol.* **2005,** *7*, 165–171.
25. Liu, K.-K.; Wang, C.-C.; Cheng, C. L.; Chao, J.-I. Endocytic Carboxylated Nanodiamond for the Labeling and Tracking of Cell Division and Differentiation in Cancer and Stem Cells. *Biomaterials* **2009,** *30*, 4249–4259.
26. Faklaris, O.; Joshi, V.; Irinopoulou, T.; Tauc, P.; Sennour, M.; Girard, H.; Gesset, C.; Arnault, J. C.; Thorel, A.; Boudou, J. P.; *et al.* Photoluminescent Diamond Nanoparticles for Cell Labeling: Study of the Uptake Mechanism in Mammalian Cells. *ACS Nano* **2009,** *3*, 3955–3962.
27. Dutta, D.; Sundaram, S. K.; Teeguarden, J. G.; Riley, B. J.; Fifield, L. S.; Jacobs, J. M.; Addleman, S. R.; Kaysen, G. A.; Moudgil, B. M.; Weber, T. J. Adsorbed Proteins Influence the Biological Activity and Molecular Targeting of Nanomaterials. *Toxicol. Sci.* **2007,** *100*, 303–315.
28. Kairdolf, B. A.; Mancini, M. C.; Smith, A. M.; Nie, S. Minimizing Nonspecific Cellular Binding of Quantum Dots with Hydroxyl-Derivatized Surface Coatings. *Anal. Chem.* **2008,** *80*, 3029–3034.
29. Verma, A.; Stellacci, F. Effect of Surface Properties on Nanoparticle−Cell Interactions. *Small* **2010,** *6*, 12–21.
30. Chao, J.-I.; Perevedentseva, E.; Chung, P.-H.; Liu, K.-K.; Cheng, C.-Y.; Chang, C.-C.; Cheng, C.-L. Nanometer-Sized Diamond Particle as a Probe for Biolabeling. *Biophys. J.* **2007,** *93*, 2199–2208.
31. Zhang, B.; Li, Y.; Fang, C. Y.; Chang, C. C.; Chen, C. S.; Chen, Y. Y.; Chang, H. C. Receptor-Mediated Cellular Uptake of Folate-Conjugated Fluorescent Nanodiamonds: A Combined Ensemble and Single-Particle Study. *Small* **2009,** *5*, 2716–2721.
32. Ruan, G.; Agrawal, A.; Marcus, A. I.; Nie, S. Imaging and Tracking of Tat-Peptide-Conjugated Quantum Dots in Living Cells: New Insights into Nanoparticle Uptake, Intracellular Transport and Vesicle Shielding. *J. Am. Chem. Soc.* **2007,** *129*, 14759–14766.
33. Jiang, W.; Kim, B. Y.; Rutka, J. T.; Chan, W. C. Nanoparticle-Mediated Cellular Response Is Size-Dependent. *Nat. Nanotechol.* **2008,** *3*, 145–150.
34. Mellman, I. Endocytosis and Molecular Sorting. *Annu. Rev. Cell. Dev. Biol.* **1996,** *12*, 575–625.
35. Martinez, G. R.; Loureiro, A. P.; Marques, S. A.; Miyamoto, S.; Yamaguchi, L. F.; Onuki, J.; Almeida, E. A.; Garcia, C. C.; Barbosa, L. F.; Medeiros, M. H.; Di Mascio, P. Oxidative and Alkylating Damage in DNA. *Mutat. Res.* **2003,** *544*, 115–127.

36. Kruger, A.; Liang, Y.; Jarre, G.; Stegk, J. Surface Functionalisation of Denotation Diamond Suitable for Biological Applications. *J. Mater. Chem.* **2006,** *16*, 2322–2328.
37. Krueger, A.; Stegk, J.; Liang, Y.; Lu, L.; Jarre, G. Biotinylated Nanodiamond: Simple and Efficient Functionalization of Detonation Diamond. *Langmuir* **2008,** *24*, 4200–4204.
38. Kruger, A.; Kataoka, F.; Ozawa, M.; Fujino, T.; Suzuki, Y.; Aleksenskii, A. E.; Ya Vul, Y.; Osawa, E. Unusually Tight Aggregation in Detonation Nanodiamond: Identification and Disintegration. *Carbon* **2005,** *43*, 1722–1730.
39. Ushizawa, K.; Sato, Y.; Mitsumori, T.; Machinami, T.; Ueda, T.; Ando, T. Covalent Immobilization of DNA on Diamond and Its Verification by Diffuse Reflectance Infrared Spectroscopy. *Chem. Phys. Lett.* **2002,** *351*, 105–108.